J Geophys (1984) 54:163–173

Journal of Geophysics

Original investigations

A paleomagnetic study of tertiary volcanics from the Hocheifel (Germany) and the cenozoic apparent polar wander path of Central Europe

Norbert Weinreich and Ulrich Bleil

Institut für Geophysik, Ruhr-Universität Bochum, Postfach 102148, 4630 Bochum 1, Federal Republic of Germany

Abstract. Paleomagnetic results are presented for 367 samples from a total of 54 igneous bodies from the Hocheifel (Germany) Tertiary volcanic province. Available radiometric age controls enable the data to be reliably assigned to the Late Eocene and predominantly to the Oligocene period. The mean virtual geomagnetic pole (VGP) position of 80.8° N, 182.0° E, $A_{95}=4.2°$ coincides perfectly with the apparent polar wander path for Eurasia in Mid-Tertiary times.

All published paleomagnetic results for other Late Oligocene to mostly Miocene centers of volcanic activity in Central Europe are reviewed. Their VGP's typically fall into the 90°–180° E longitudinal quadrant (mean: 78.7° N, 141.9° E, $A_{95}=4.4°$). Together with pole positions for Lower Tertiary North European volcanic provinces (mean: 79.1° N, 171.1° E, $A_{95}=6.3°$) they result in a rather complex apparent polar wander relative to Western Europe during the Tertiary era which, according to the presently available data, would differ significantly from the APW path for the Russian/Siberian platform.

Key words: Paleomagnetism – Central European Tertiary volcanism – Apparent polar wander path

Introduction

The Eifel volcanic fields are the westernmost link in a roughly straight chain of Cenozoic Central European volcanic provinces extending eastward for some 700 km to Silesia, approximately along latitude 50.5° N. Duncan et al. (1972) postulated the existence of a hotspot ('Eifel plume') beneath the eastward moving European plate successively feeding the various volcanic centers since about Mid-Oligocene. Abundant radiometric age data published during the last decade, however, do not support their hypothesis of an almost continuous progressive decrease in age along the volcanic belt from east to west (see review by Lippolt, 1982). Instead, there is compelling evidence that several synchronous eruptive phases took place between Late Eocene and Quaternary without any apparent systematic spatial relationship.

Moreover, the assumption of a single E-W trending volcanic arc is certainly somewhat arbitrary as there are a number of Cenozoic volcanic centers of different ages both to the north and to the south, around and within the Upper Rhinegraben and its NE branch into Lower Hesse and Lower Saxony. In fact, the formation of the Rhinegraben rift system and the subsequent regional uplift of the Rhenish shield is suggested as a potential tectonic mechanism contributing to magma generation in the Eifel and adjacent areas (Illies et al., 1979). Duda and Schmincke (1978) generalized this aspect by associating mass movements in the mantle, related to the Alpine folding, to an uplift and magmatic activity along the Central European volcanic chain running roughly parallel, some 300 km to the north of the Alpine fold belt.

Paleomagnetic studies have been published for almost all Tertiary volcanic provinces in Central Europe. Their review shows that on modern standards some of these data sets are at best fragmentary. Previous paleomagnetic work in the Eifel region has been concentrated mainly on the Quaternary volcanic fields of the Lake Laach area in the east (Kohnen and Westkämper, 1978; Böhnel et al., 1982) and the Maar district in the west (Haverkamp, 1980; Jäger, 1982). Both these eruptive phases show little overlap in space with a precursory, at least as intense, volcanic activity in the central part, the Hocheifel (Fig. 1). Here, K/Ar ages range from 45 to 23 m.y. (Cantarel and Lippolt, 1977). A preliminary paleomagnetic survey on 8 dated volcanic bodies was published by Bleil et al. (1982). These authors also discussed rock magnetic and magneto-mineralogical properties. For one Tertiary volcano a remanent magnetization direction was determined by Nairn (1962) and Böhnel et al. (1982). The main aim of this study is to present a complete paleomagnetic analysis of the Hocheifel volcanics.

Geologic setting

The 'Rheinisches Schiefergebirge' (Rhenish Slate Mountains) is an uplifted plateau composed of a thick series of mainly Devonian and Lower Carboniferous slates, greywackes and quartzites. In its northwestern part, the Hocheifel region, a suite of volcanic rocks pierces those strata which were strongly folded during the Hercynian orogeny. Within an area of about 500 km^2, more than 130 eruptive centers have been identified (Knetsch, 1959). Their ages range from Middle Eocene to Late Oligocene (Cantarel and Lippolt, 1977) and mark the earliest volcanic activity within the central Rhenish shield.

The rocks consist of alkali basalts, grading by mode and chemistry towards hawaiites, mugearites and trachytes (Huckenholz, 1965a). The available K/Ar ages indicate an initial andesitic phase limited to Eocene times followed by

Offprint requests to: U. Bleil

Table 1. Summary of sampling sites

Site	Locality	Geographic coordinates (°N/°E)	Rock type	Age (m.y.)
AB	Alte Burg	50.397/6.892	basanite(3)	
BM	am Booser Maar	50.308/6.992	alkali olivine basalt(2)	37(8)
GK	am Gewader Köpfchen	50.303/6.950	alkali basalt(6)	
AS	am Selberg	50.337/6.947	alkali basalt(6)	
VH-I	am Vogelsherdchen I	50.348/6.958	alkali basalt(6)	
VH-II	am Vogelsherdchen II	50.348/6.958	alkali basalt(6)	
AR	Arensberg	50.290/6.732	basanite(5)	24/32(7) 23(8)
HS	Auf der Hurstatt	50.237/6.912	alkali basalt(6)	
BA	Barsberg	50.295/6.848	alkali basalt(6)	36(9)
BS	Beilstein	50.287/6.972	alkali basalt(6)	
BB	Bereborn	50.283/6.962	alkali basalt(6)	
MU	Bocksberg I	50.320/6.925	oligo andesite(1)	43(7),18(9)
BO	Bocksberg II	50.320/6.925	oligo andesite(1)	
KO	Brinkenköpfchen	50.275/6.938	oligo andesite(1)	41(7)
BK-I	Burgkopf I	50.370/6.808	basanite(6)	
BK-II	Burgkopf II	50.370/6.808	basanite(6)	
CO	Cotenickelchen	50.332/6.953	alkali basalt(6)	
DK	Die Kapp	50.230/6.892	alkali basalt(6)	
DL	Düngerlei	50.370/6.805	alkali basalt(6)	
FR	Freienhäuschen	50.272/6.938	trachyte(1)	
GA	Galgenkopf	50.355/6.982	alkali basalt(6)	
GL	Gefell	50.238/6.908	basanite(5)	
GE	Gewaderköpfchen	50.303/6.950	mugearite(2)	33(7)
HK	Hochkelberg	50.275/6.953	picrite basalt(4)	41(9)
HO-I	Höchstberg I	50.240/7.042	alkali olivine basalt(5)	
HO-II	Höchstberg II	50.235/7.040	alkali olivine basalt(5)	34(7)
HO-III	Höchstberg III	50.240/7.040	alkali olivine basalt(5)	
HA	Hohe Acht	50.387/7.012	ankaramite(4)	38(7)
GB	Hoch-Bermel	50.282/7.095	basanite(3)	
HB	Holzberg	50.298/6.978	picrite basalt(3)	
HN	Hünerbach	50.288/6.950	trachyte(2)	
HU	Hüstchen	50.328/6.937	alkali basalt(6)	
JH	Jonashübel	50.188/6.967	leuco trachyte(2)	
KA	Karnickelchen	50.272/6.937	oligo andesite(1)	42(7)
KB	Kleiner Bermel	50.280/6.087	basanite(3)	
KH	Kölnische Höfe	50.230/7.030	basanite(5)	
LI	Liers	50.462/6.945	alkali basalt(6)	
MH	Maihöchstchen	50.280/6.938	picrite basalt(4)	
MB	Michelsberg	50.512/6.822	alkali basalt(6)	
NS	Nitzbachsteinchen	50.387/6.948	basanite(4)	
NB-I	Nürburg I	50.347/6.953	basanite(3)	34(7)
NB-II	Nürburg II	50.338/6.953	basanite(3)	
RL	Rappoldsley	50.367/6.938	hawaiite(2)	
RA	Raustert	50.330/6.970	oligo andesite(1)	45(7)
RE	Reimerath	50.308/6.958	leuco trachyte(1)	41(7)
RO	Rotläufchen	50.238/7.062	basanite(5)	
SK	Scharfer Kopf	50.330/6.938	alkali olivine basalt(2)	
SC	Schule Nerdlen	50.230/6.867	alkali basalt(6)	
SE	Selberg	50.347/6.937	phonolite(2)	30(7)
SM	Steimelskopf	50.233/7.005	alkali olivine basalt(5)	
ST	Steinkäulchen	50.292/6.967	alkali trachyte(1)	
HT	südlich Hütchesberg	50.230/6.925	alkali basalt(6)	
SR	südlich Reimerath	50.298/6.953	alkali basalt(6)	
VO	Vogelsherdchen	50.353/6.955	alkali basalt(6)	

(1) Grünhagen, 1964; (2) Huckenholz, 1965a; (3) Huckenholz, 1965b; (4) Huckenholz, 1966; (5) Chauduri, 1970; (6) Huckenholz, pers. comm. 1981; (7) Cantarel and Lippolt, 1977; (8) Schmincke and Mertes, 1979; (9) Lippolt and Fuhrmann, 1980 (unpublished data)

basaltic and basanitic eruptions during Oligocene. Trachytes apparently were emplaced more or less over the entire period of volcanic activity.

Volcanic edifices have generally been eroded, most present occurrences representing subvolcanic feeder conduits. The samples for this paleomagnetic study were obtained mainly from formerly quarried stocks and necks, now prominent features within the landscape of a deeply eroded Paleozoic environment.

Materials and methods

A total of 54 sites were sampled for the present paleomagnetic study. Cores (2.5 cm in diameter, 5–15 cm long) were

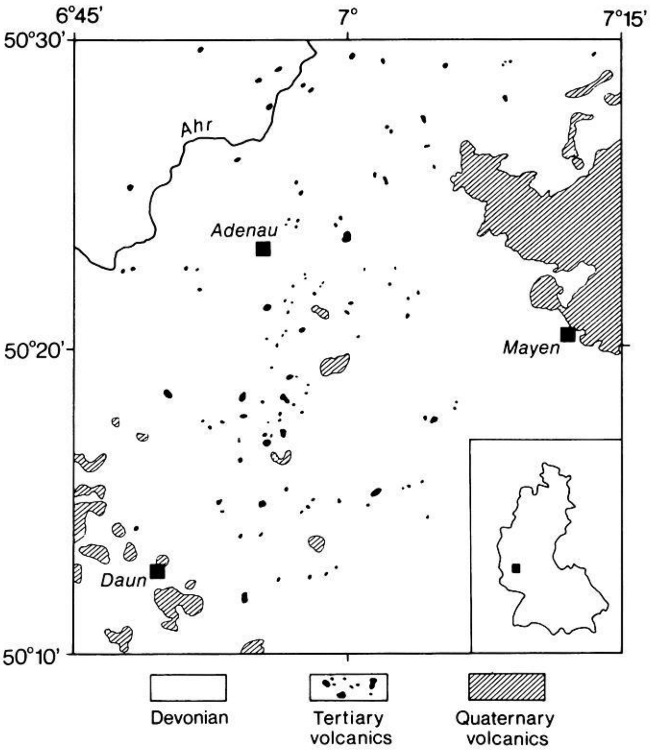

Fig. 1. Geologic sketch map of the central Eifel area

drilled and their orientation taken in situ with a magnetic and/or sun compass before removal from the outcrop. Whenever possible, a representative sampling was attempted by taking 5 or more individual cores over the greatest practicable distance at each site.

Table 1 summarizes the basic sampling-site information. Besides geographic coordinates of the localities, the respective rock types and, where available K/Ar ages are listed.

For the magnetic analyses the cores were cut into standard-sized 2.5 cm long specimens. All measurements of the magnetization directions and intensities were made on a Digico spinner magnetometer. For the alternating field (AF) demagnetization treatment a Schonstedt GSD-1 single axis demagnetizer was used. The susceptibilities were determined by means of a Bison 3101A bridge.

A systematic AF demagnetization was carried out on at least one pilot specimen per site. According to their results, an optimum, generally less detailed demagnetization procedure was established for the bulk of the material. Stable magnetization directions were evaluated from different graphical representations of the demagnetization data illustrating the changes in direction and intensity of remanence:

(a) demagnetization curves, giving the intensity variation normalized to the initial natural remanent magnetization, NRM as function of the demagnetizing fields (Figs. 2a and 3a);

(b)vector diagrams of the orthogonal magnetization components (Zijderveld, 1967) after each demagnetization step (Figs. 2b and 3b);

(c) stereographic plots of the resultant vectors, the directions remaining upon progressive demagnetization (Figs. 2c and 3c);

(d) stereographic plots of the difference vectors (Hoffman and Day, 1978), the directions removed upon progressive demagnetization (Figs. 2d and 3d).

The stable direction, corresponding to the primary characteristic remanent magnetization, ChRM, was determined for each specimen from the demagnetization interval yielding the least directional scatter. The site mean ChRM directions are calculated from sample means and defined on basis of minimum circles of confidence and maximum precision k-parameters.

Natural remanent magnetization, NRM

The NRM site mean directions generally cluster around the centered axial dipole direction of the sampling area (Fig. 4a). Mostly, a moderate within-site scatter is observed, at about 25% of the sites, however, α_{95} exceeds 20° (Table 2). The NRM intensities vary between about 0.1 and 20 A m^{-1}. There is no obvious correlation of the magnetization intensities and susceptibilities with the petrology of the rocks, only trachytes consistently gave conspicuous low values for both parameters. On the other hand, remarkably different NRM intensities were found for normal polarities – geometric mean 5.6 A m^{-1} – and reversed polarities – geometric mean 2.7 A m^{-1} –. Almost identical susceptibility mean values of 3.4 10^{-2} SI units for both collections indicate that the contrasting remanent intensities result from the magnetization history rather than from intrinsic magnetic properties of the rocks. For about 25% of the sites, and most always coinciding with extremely high α_{95} for the NRM directions, the Koenigsberger ratios were found to be less than unity.

Demagnetization experiments

For each sampling site at least one pilot specimen was systematically demagnetized in alternating fields. Up to 20 mT AF increments of 2 mT were applied, between 20 and 40 mT the demagnetization steps were increased to 5 mT and beyond this stage to 10 mT or more. The demagnetization process was pursued until the remaining remanence was clearly single-component and a stable characteristic remanent magnetization, ChRM, could be unequivocally determined. The evaluation of the ChRM data was done by means of combined graphical methods (Figs. 2 and 3).

The samples frequently contain unstable spurious magnetization components which are entirely removed at low demagnetization stages of 10 mT or less. Mostly their presence is clearly evident only from the vector difference graphs (Fig. 2d), in some rare cases, where they hold larger fractions of the total remanence, they cause a more distinct directional variation upon demagnetization which also can be traced in the Zijderveld diagrams and resultant vector graphs. Although it appears that the declinations are generally more sensitive to this kind of secondary magnetization, they do not show any consistent grouping. A likely interpretation, therefore, would be a random overprinting during sampling and/or subsequent storage and handling in the laboratory.

The quantification or even identification of viscous remanent magnetization, VRM, components is very limited for samples carrying a normal ChRM due to the directional similarity of the present Brunhes field and the former Tertiary fields. In contrast, for almost all samples yielding a reversed ChRM the demagnetization process revealed a more or less pronounced VRM component. Figure 3 summarizes the most typical features of this behavior. The removal of a roughly antiparallel VRM results in only minor changes of the resultant remanent direction over the whole demagnetization process (Fig. 3c). Their effect, however, becomes very obvious in the demagnetization curve

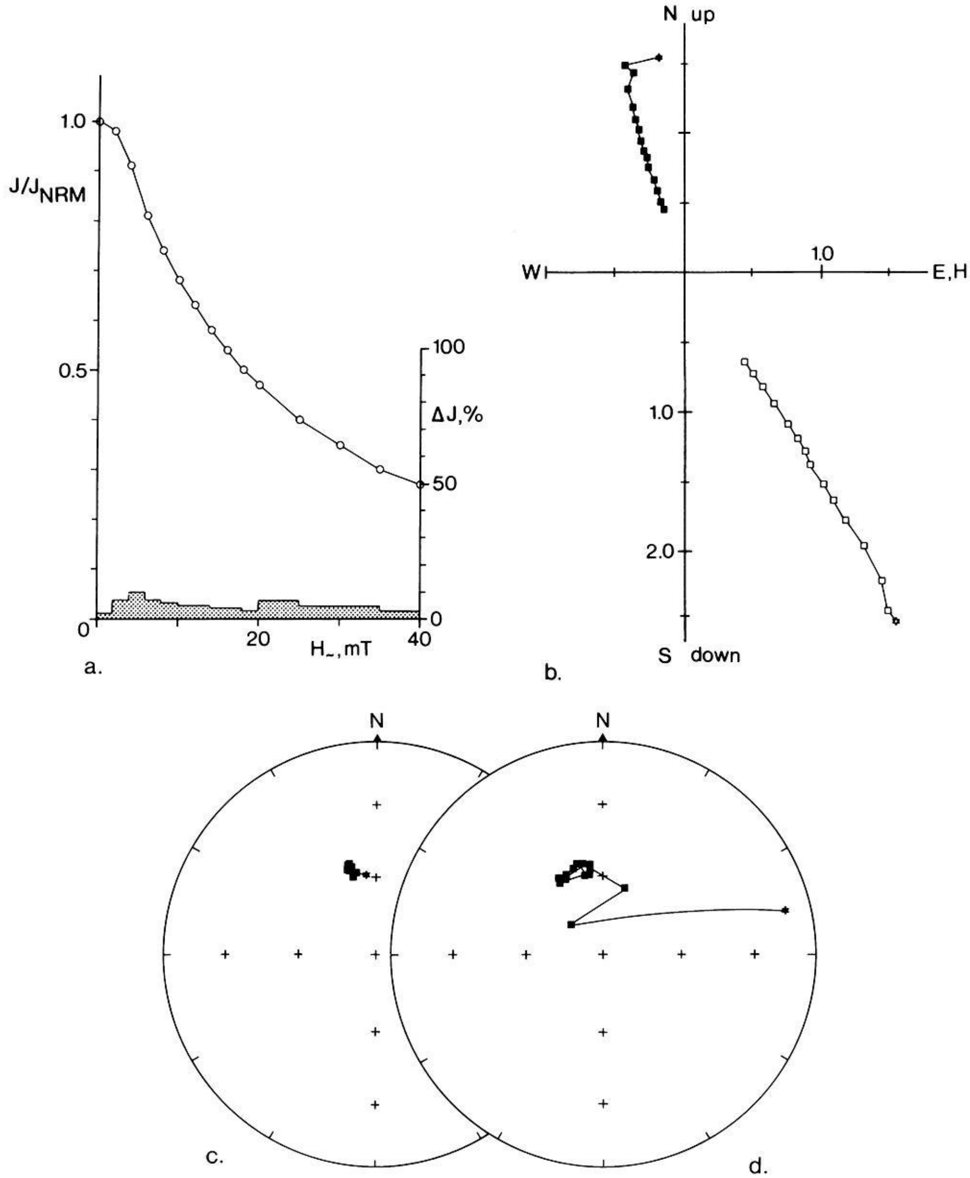

Fig. 2a–d. AF demagnetization characteristics of pilot sample Hoch-Bermel (GB-I). **a** Intensity of NRM normalized remanent magnetization as function of the applied demagnetizing field and variation of remanent intensity in per cent for each demagnetization step (*dotted*). **b** Vector diagram illustrating the changes in direction and intensity (in A m^{-1}) of remanence during progressive demagnetization. *Solid* and *open* symbols represent declination and inclination, respectively. The stars give the NRM directions. AF increments can be read from Fig. 2a. **c** Stereographic projection of the resultant vectors of magnetization. *Closed* symbols indicate positive, *open* symbols negative inclinations, respectively. The star gives the NRM direction, all directions are connected by great-circles. AF increments can be read from Fig. 2a. **d** Stereographic projection of the difference vectors. *Closed* symbols indicate positive, *open* symbols negative inclinations, respectively. The *star* gives the first demagnetization step, all directions are connected by great-circles. AF intervals can be read from Fig. 2a

(Fig. 3a). Both here and in the Zijderveld diagram (Fig. 3b) an apparent increase of the total remanent intensity and their respective orthogonal components indicate that a relatively unstable remanence of normal polarity is destroyed by the AF treatment up to about 15 mT while a stable remanence of reversed polarity remains essentially unchanged. The vector difference graph (Fig. 3d) suggests that the unstable component is in fact of viscous origin as up to alternating fields of 10 mT the directions of the eliminated remanences cluster closely around the Brunhes field for the sampling site. Between about 10 and 20 mT, the difference vectors show intermediate directions which gradually approach the ChRM direction. In this interval, therefore, the stability fields of the primary and secondary magnetizations overlap. Beyond about 20 mT, the VRM is completely erased, the remaining remanence is essentially single-component and upon further demagnetization to 100 mT, the directions of resultant and difference vectors, on average, coincide.

Characteristic remanent magnetization, ChRM

According to the results obtained by the AF treatment of the pilot specimen, all samples of a site were progressively demagnetized over an appropriate interval of several tenths of mT. From these data a ChRM direction was then determined for each sample. The site mean ChRM directions together with statistical parameters and the respective pole positions are summarized in Table 2. It shows that the large scatter observed in the NRM of many sites could be drastically reduced by the demagnetization process and, with but a few exceptions, α_{95} of the order of 5° are typical for the ChRM results.

At four sites (Brinkenköpfchen, KO; Höchstberg, HO-II; Rappoldsley, RL; Steimelskopf, SM) pole positions of less than 45° latitude were obtained. These data, therefore, are not included in any further mean calculation. Whether they represent true transitional paleofield configurations can not be decided on basis of the present results. Ryall et al. (1977) have pointed out that the recording of geomagnetic transitions or excursions by an episodic volcanism is statistically very improbable. Analyses of a great number of Icelandic lava flows showed that only about 5% had recorded a transitional field state.

Site HO-II belongs to a large volcanic complex now quarried in several outcrops. The two other sites sampled here, HO-I and HO-III, both gave similar, but apparently

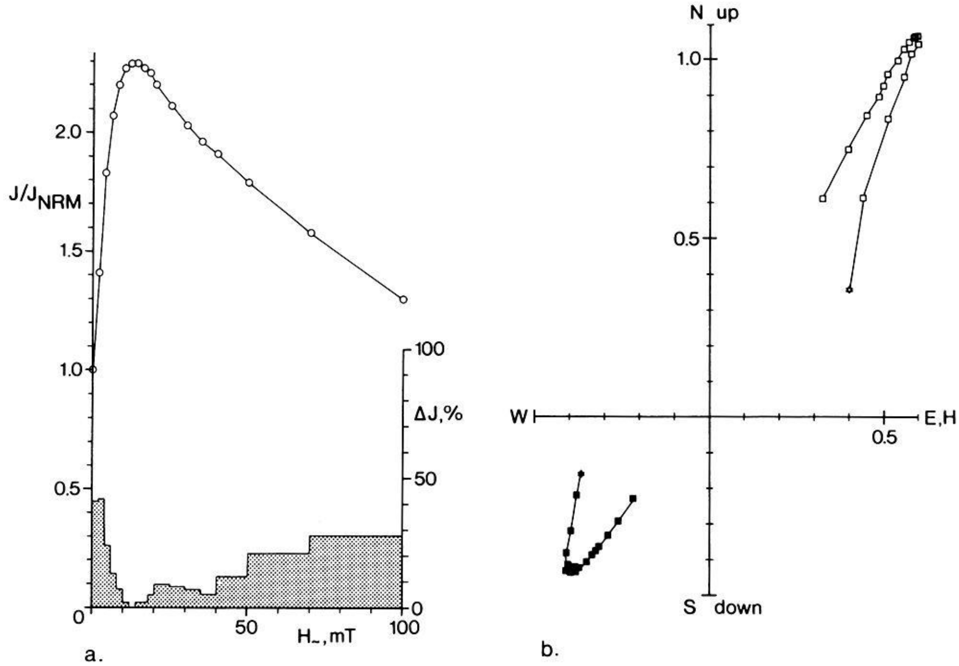

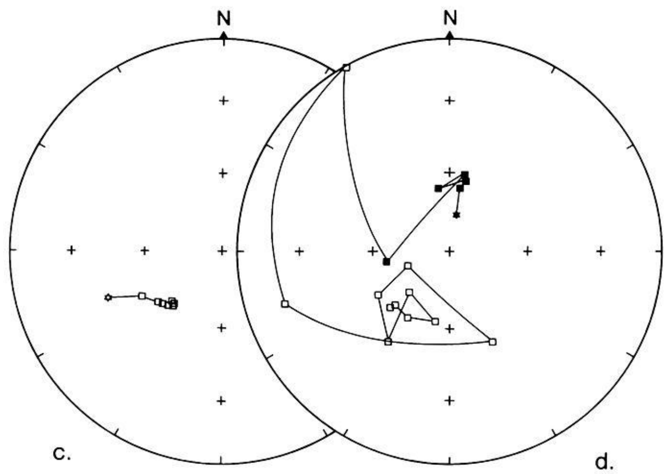

Fig. 3a–d. AF demagnetization characteristics of pilot sample Freienhäuschen (FR-I/1). See caption of Fig. 2 for details

not identical, normal directions. This implies that the volcanic activity prevailed at least over a period of some 10^2 years. A possible explanation for the erratic ChRM direction of site HO-II, therefore, would be a volcano-tectonic fragmentation and dislocation of older parts of the volcanic edifice upon subsequent eruptions. To an unknown extent such effects may also have affected a number of other sites sampled for this study. However, due to the complete absence of any useful horizontal reference features, nowhere a bedding correction could be applied.

As for the Höchstberg sites, the two outcrops sampled at the Nürburg (NB-I, NB-II) also gave significantly different ChRM directions. Two adjacent sites am Vogelsherdchen (VH-I, VH-II) even revealed opposite remanent magnetization polarities. A time span of at least 10^4 years should thus separate consecutive volcanic pulses at this locality. On the other hand, within three volcanic complexes (Bocksberg, BO and MU; Burgkopf, BK-I and BK-II; Gewaderköpfchen, GE and GK) the stable remanent magnetization directions of different sampling sites on grounds of overlapping α_{95} and positive F-tests are identical. Their respective data have been combined to common mean values for these volcanoes.

As evident from Table 2 and Fig. 4b, a number of sites, both of normal and reversed ChRM polarity, without any obvious spatial relation, yield very similar, stable paleomagnetic directions. Although it may be tempting to assign a contemporaneous volcanic activity here, such a conclusion would only be justified with additional, convincing and independent proof. The mere fact of coinciding or very similar paleomagnetic directions in different rock units of the same geologic period in a given area can of course result from an approximately synchronous acquisition of their remanent magnetizations but with at least the same probability, their ages may be different by up to many million years (see e.g. the data of sites Arensberg, AR and Hohe Acht, HA, Tables 1 and 2). On the other hand, clearly different ChRM directions reflecting a regular paleosecular field variation can be obtained from volcanic rocks which were emplaced within only a few 10^2 years. Even for opposite magnetization polarities the minimum age difference is only of the order of 10^4 years, the time required for the Earth's magnetic field to complete a reversal (Fuller et al., 1979).

It is interesting to note in this context that for volcanic structures with similar K/Ar ages (Table 1) the same ChRM polarity was always observed. Thus the five sites (Bocksberg, BO, MU; Brinkenköpfchen, KO; Hochkelberg, HK; Karnickelchen, KA; Reimerath, RE) giving radiometric ages of 41–43 m.y. carry a reversed magnetic polarity which may tentatively be correlated to the reversed interval between marine magnetic anomalies 18 and 19 (Ness et al., 1980). Similarly, the three sites of normal polarity (am Booser Maar, BM; Barsberg, BA; Hohe Acht, HA) with K/Ar ages of 36–38 m.y. could represent the mostly normal periods of marine anomalies 15 and 16. However, another three sites of normal polarity (Gewaderköpfchen, GE, GK; Höchstberg, HO-I, HO-II, HO-III; Nürburg, NB-I, NB-II) gave K/Ar ages of 33–34 m.y. which fall into the long reversed interval between marine anomalies 12 and 13.

At site Arensberg, AR, Fuchs (1969) on the basis of geologic field observations has distinguished two eruptional phases for which Cantarel and Lippolt (1977) determined radiometric ages of 32 and 24 m.y., respectively. Only the

Table 2. Summary of paleomagnetic results from Tertiary Hocheifel volcanics

Site	*N*	NRM				ChRM					Pole Position			
		J_{NRM}	*D*	*I*	α_{95}	*D*	*I*	*k*	*R*	α_{95}	λ'	ϕ'	*dp*	*dm*
AB	7/7	0.99	163.1	−32.0	28.9	167.8	−53.7	316	6.98	3.4	71.7	220.3	3.5	4.8
BM	6/6	18.90	347.8	+47.4	4.5	350.8	+71.7	661	5.99	2.6	83.1	330.7	4.0	4.5
GK	5/5	4.81	337.7	+68.2	10.3	355.6	+62.3	469	4.99	3.5	82.8	212.8	4.3	5.5
AS	6/6	4.32	27.5	+65.7	4.4	4.3	+62.8	386	5.99	3.4	83.3	159.0	4.2	5.4
VH-I	4/4	7.40	356.0	+72.7	10.4	10.2	+77.8	256	3.99	5.8	72.9	19.1	10.2	10.8
VH-II	6/6	5.03	153.1	−73.7	6.3	171.4	−71.4	107	5.95	6.5	82.2	328.5	10.0	11.4
AR*	18/18	5.46	3.7	+55.1	8.8	1.2	+55.1	239	17.93	2.2	75.3	183.1	2.2	3.1
HS	6/6	4.26	10.5	+63.1	2.1	5.0	+54.9	714	5.99	2.5	74.9	170.8	2.5	3.6
BA	6/4	7.00	60.0	+44.6	66.0	2.5	+39.2	33	3.91	16.2	62.0	181.6	11.6	19.4
BS	6/5	2.69	340.6	+55.2	15.0	342.7	+50.9	85	4.95	8.3	67.4	227.8	7.6	11.2
BB	5/5	6.37	351.3	+44.9	8.8	345.3	+41.2	103	4.96	7.6	61.1	215.3	5.6	9.2
MU*	16/16	0.54	336.5	−34.6	29.4	203.3	−75.9	103	15.86	3.6	72.1	42.0	6.1	6.6
BO	5/4	0.42	358.0	−9.3	>90	201.0	−72.1	76	3.96	10.4	75.9	60.2	16.5	18.7
MU/BO	−/20	−	−	−	−	205.5	−75.2	98	19.81	3.3	71.1	46.8	5.5	6.1
KO*	11/11	2.10	269.4	−44.2	60.6	249.7	−62.8	47	10.79	6.7	44.1	76.3	8.2	10.5
BK-I	5/5	8.71	353.2	+53.3	6.9	349.1	+51.1	125	4.97	6.9	69.9	214.3	6.3	9.3
BK-II	5/5	6.20	353.9	+57.0	5.2	351.8	+52.4	230	4.98	5.1	71.7	208.9	4.8	7.0
BK-I/II	−/10	−	−	−	−	351.9	+51.8	172	9.95	3.7	71.1	208.5	3.4	5.0
CO	7/7	3.57	155.3	−61.9	10.0	165.8	−67.0	304	6.98	3.5	80.9	278.7	4.8	5.8
DK	6/6	3.56	272.9	+21.5	34.0	8.6	+47.1	63	5.92	8.5	67.2	166.7	7.1	11.0
DL	6/6	7.92	1.1	+65.1	2.7	357.1	+63.9	622	5.99	2.7	85.0	210.3	3.4	4.3
FR	5/5	0.49	206.3	−28.1	20.4	196.7	−58.1	72	4.95	9.1	73.6	134.1	9.9	13.4
GA	6/5	5.41	12.4	+55.9	7.5	11.7	+54.5	135	4.97	6.6	72.6	152.9	6.6	9.3
GL	6/6	2.58	207.3	−51.5	9.9	214.9	−62.2	133	5.96	5.8	65.5	98.7	7.1	9.1
GE*	16/14	4.33	348.4	+57.0	5.8	349.9	+59.6	107	13.88	3.9	77.8	226.2	4.4	5.8
GK/GE	−/19	−	−	−	−	351.7	+60.3	127	18.86	3.0	79.3	222.6	3.4	4.5
HK	6/6	3.12	191.0	−48.6	10.7	196.4	−49.6	453	5.99	3.2	66.8	148.5	2.8	4.2
HO-I	6/5	3.57	350.6	+55.1	13.4	354.7	+52.0	119	4.97	7.0	72.0	201.6	6.6	9.6
HO-II	6/6	2.34	65.5	+62.5	12.7	76.8	+38.3	30	5.83	12.5	24.7	92.5	8.8	14.8
HO-III*	12/12	2.01	288.8	+48.3	26.8	341.2	+50.0	98	11.98	4.4	65.9	229.7	3.9	5.9
HA*	10/10	2.43	353.9	+49.0	4.4	9.3	+51.4	418	9.98	2.3	70.5	162.8	2.1	3.1
GB	5/5	3.04	341.6	+59.2	5.0	341.3	+56.4	192	4.98	5.5	71.2	239.6	5.8	8.0
HB	6/5	0.58	82.9	+ 2.0	50.0	147.1	−66.7	229	4.98	5.1	68.9	286.9	6.9	8.4
HN	4/4	1.43	8.0	+58.1	3.9	14.8	+48.5	311	3.99	5.2	66.5	152.7	4.5	6.9
HU	8/8	4.41	6.0	+62.2	9.2	7.4	+64.9	157	7.96	4.4	84.1	127.9	5.8	7.1
JH	6/6	0.37	93.6	+76.4	13.6	156.9	−39.3	121	5.96	6.1	56.7	228.0	4.4	7.3
KA	6/6	1.34	170.7	−43.1	19.2	199.8	−65.0	95	5.95	6.9	77.8	104.8	9.0	11.1
KB	5/5	3.40	358.8	+63.0	6.5	351.8	+64.3	306	4.99	4.4	83.2	243.6	5.6	7.0
KH	5/4	8.39	2.3	+67.1	13.0	346.4	+62.2	580	4.00	3.8	78.6	246.6	4.6	5.9
LI	5/5	3.71	211.3	−49.7	4.1	199.1	−53.8	1594	5.00	1.9	68.8	138.1	1.9	2.7
MH	6/4	1.48	293.7	+60.8	32.1	353.5	+76.5	182	3.98	6.8	75.5	355.6	11.7	12.6
MB	5/5	0.12	8.4	+29.3	7.9	7.4	+29.6	111	4.96	7.3	54.6	174.1	4.4	8.0
NS	7/7	9.35	282.2	+46.5	17.6	334.4	+66.3	268	6.98	3.7	73.4	281.3	5.0	6.1
NB-I	6/6	5.83	343.1	+69.1	24.7	0.6	+61.5	212	5.98	4.6	82.4	183.2	5.5	7.1
NB-II	6/6	4.28	34.2	+58.1	7.1	33.0	+51.9	358	5.99	3.5	60.0	120.0	3.3	4.8
RL	6/4	2.48	147.1	+47.9	15.5	142.0	−16.7	52	3.94	12.9	37.8	237.1	6.9	13.3
RA*	13/13	1.26	176.3	−67.7	5.5	183.1	−70.1	405	12.97	2.0	85.7	31.8	3.0	3.5
RE	5/5	0.11	188.8	−59.9	21.5	192.6	−60.8	275	4.99	4.6	77.9	135.6	5.4	7.1
RO	6/6	8.03	6.7	+59.8	2.7	6.2	+57.3	368	5.99	3.5	77.0	164.8	3.7	5.1
SK	5/5	13.49	188.8	−66.9	5.8	189.3	−66.2	216	4.98	5.2	83.7	107.9	7.0	8.6
SC	6/6	2.92	350.0	+57.6	6.1	352.2	+52.1	224	5.98	4.5	71.6	207.8	4.2	6.2
SE*	11/11	0.61	358.5	+55.4	8.2	357.4	+64.5	203	10.95	3.2	85.6	211.3	4.1	5.1
SM	5/4	4.73	63.3	+11.6	29.7	51.8	+15.3	185	3.98	6.8	29.7	123.3	3.6	7.0
ST	3/3	8.33	98.3	+35.7	78.1	23.0	+55.2	96	2.98	12.7	69.4	125.7	13.5	18.5
HT	5/5	8.31	358.2	+61.5	23.8	346.6	+68.3	92	4.96	8.0	81.4	290.6	11.4	13.5
SR	6/5	4.42	28.7	+61.7	8.1	30.8	+57.5	471	4.99	3.5	65.1	113.6	3.8	5.2
VO	7/7	6.26	359.2	+57.8	9.7	351.8	+49.4	118	6.95	5.6	69.1	206.8	4.9	7.4

N number of samples in NRM/ChRM mean; J_{NRM} geometric mean NRM intensity in A m^{-1}; *D* declination in ° E; *I* inclination, positive downward; *k* precision parameter; *R* resultant of *N* unit vectors; α_{95} radius of the 95% confidence circle; λ', ϕ' geographic latitude in ° N and longitude in ° E of the virtual geomagnetic pole; *dp, dm* semiaxis of the 95% oval of confidence.

* Data from Bleil et al., 1982

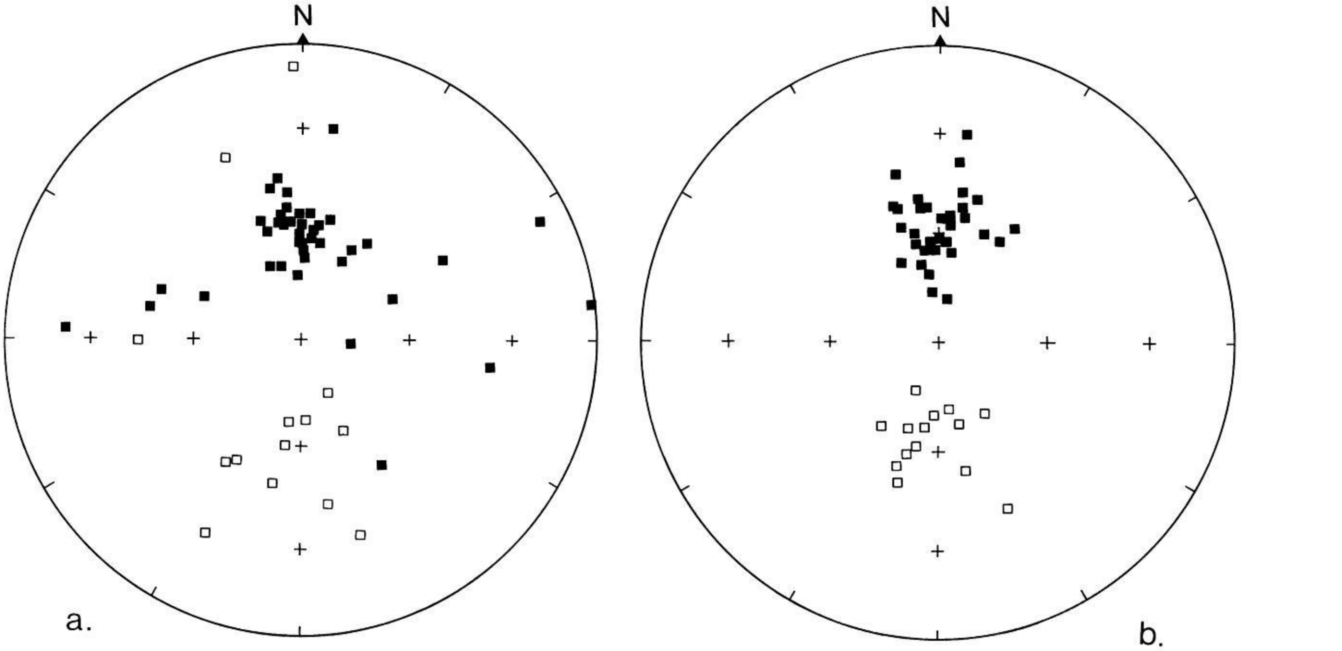

Fig. 4a and b. Site mean paleomagnetic directions of the **a** natural remanent magnetization, NRM **b** characteristic remanent magnetization, ChRM for Tertiary volcanics of the Hocheifel area (present axial geocentric dipole inclination: +67.5°). *Closed* and *open* symbols indicate positive and negative inclinations, respectively

Table 3. Average paleomagnetic directions and virtual geomagnetic pole positions for the Tertiary Hocheifel volcanics

Mean directions	N	D	I	k	R	α_{95}
Normal polarities	33	359.9	+57.5	42	32.23	3.9
Reversed polarities	14	184.1	−62.8	36	13.64	6.7
All sites[a]	47	1.0	+59.1	39	45.83	3.4
Pole positions (° N, ° E)						
	N	λ'	ϕ'	k	R	A_{95}
Normal polarities	33	79.1	188.2	28	31.86	4.8
Reversed polarities	14	84.2	153.3	21	13.37	8.9
All sites	47	80.8	182.0	25	45.17	4.2

[a] For the overall mean calculation, reversed polarities are inverted to their northern hemisphere equivalent directions. All symbols as in Table 2

latter age, however, was confirmed by Schmincke and Mertes (1979). The paleomagnetic sampling comprised both rock units and according to the extremely tight grouping of the stable remanent magnetization directions of all samples (Table 2), it appears rather unlikely that their emplacement was discontinuous over a very long period of time.

Mean directions and pole positions

Table 3 summarizes the average paleomagnetic directions and virtual geomagnetic pole (VGP) positions obtained for the Tertiary Hocheifel volcanics. The data are based on 47 individual site means. As discussed above, from a total of 54 sampling sites, 4 were omitted because of an apparent transitional field record ($\lambda' < 45°$ acceptibility criterion). For three sets of data the results of two different outcrops at a volcanic body have been combined to a common mean.

The respective mean directions for 33 sites of normal and 14 sites of reversed polarity deviate by only a small, statistically insignificant amount (Fig. 5). The observed

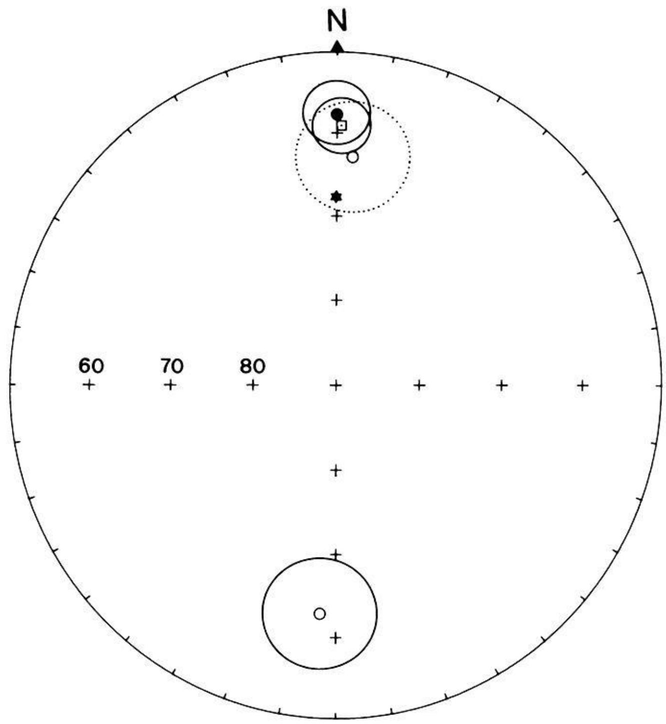

Fig. 5. Mean characteristic remanent magnetization directions with 95% circles of confidence for the Tertiary Hocheifel volcanics. *Closed circle*: mean direction of normal polarities ($N=33$); *open circle*: mean direction of reversed polarities ($N=14$) also shown as an equivalent direction on the northern hemisphere (dotted circle of confidence); *square*: mean direction of all sites; *star*: present axial geocentric dipole field direction for the Hocheifel area. 50°–90° Schmidt equal area projection

slightly shallower normal mean inclination is not compatible with an incompletely erased secondary viscous magnetization of Brunhes field origin (Pohl and Soffel, 1977). Instead, a more likely explanation would be the recording of sufficiently large and asymmetric long-term non-dipole field components (Wilson, 1970; Coupland and Van der Voo, 1980). Whatever the cause, in the inclination, the overall mean direction is significantly different from the axial geocentric dipole field for the present latitude of the Hocheifel area.

The mean pole positions for the northern hemisphere are calculated from the VGP's determined individually for each site (Table 2). A VGP derived from the mean direction of all sites is listed in Table 4 and will be discussed together with paleomagnetic data for the other Cenozoic Central European volcanic provinces in the following review.

Apparent polar wander path for Cenozoic Central Europe

The most comprehensive compilation of paleomagnetic results for all major continental blocks since the Devonian has been published by Irving (1977). The apparent polar wander (APW) path relative to northern Eurasia for the last 80 m.y. based on these data is shown in Fig. 6. The mean pole position for the Tertiary Hocheifel volcanics determined in this study falls about midway between the 30 and 40 m.y. VGP's of Irving. This result strongly supports the available radiometric ages of a predominantly Oligocene volcanic activity in this region. An especially interesting feature is the close agreement seen in the VGP longitudes. They indicate an apparent polar wander path along about the 180° meridian for the entire Cenozoic, and, neglecting true polar wander, imply a northward continental motion without a notable rotational component during this period.

However, there is a significant discrepancy of some 30° in longitude between these results and an APW compiled for stable continental Western Europe by McElhinny (1973) His Upper Tertiary pole (80° N, 157° E) is almost exclusively derived from paleomagnetic data of various Central Eu-

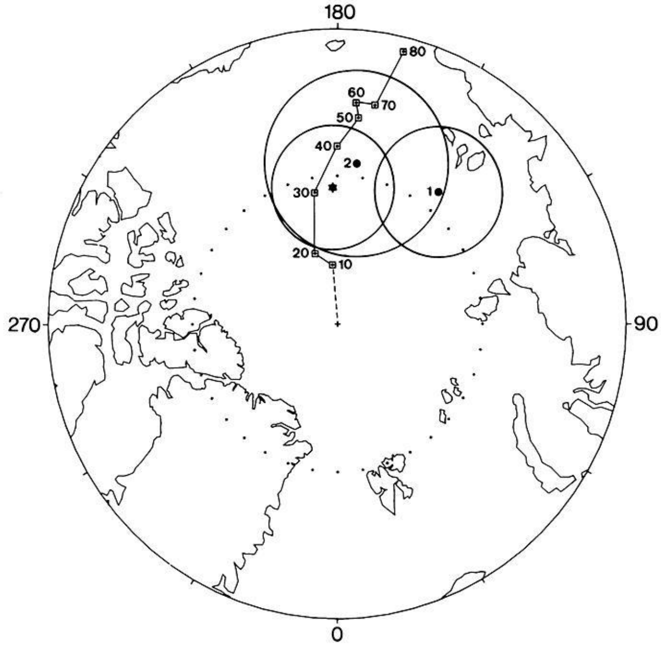

Fig. 6. Apparent polar wander path relative to Eurasia since the Late Cretaceous (Irving, 1977). *Star*: Mean virtual geomagnetic pole (VGP) for the Tertiary Hocheifel volcanics with 95% circle of confidence as determined in this study. *Closed circles*: 1) Mean Miocene VGP with 95% circle of confidence as derived from paleomagnetic data for the Central European volcanic provinces (Table 4). 2) Mean Paleocene/Eocene VGP with 95% circle of confidence as derived from paleomagnetic data for the North European, mainly British Lower Tertiary volcanic provinces (Irving et al., 1976, see text for details). 70°–90° polar projection

Table 4. Summary of age data and paleomagnetic results for Cenozoic Central European volcanics

Epoch	Volcanic center	Age	n/N	ChRM			Pole Position				References
	λ/ϕ			D	I	α_{95}	λ'	ϕ'	dp	dm	
Paleocene/ Eocene	Northern Rhinegraben Borders 49.8/8.6	65–39	8/46	10.0	60.9	14.3	79.5	143.1	16.8	21.9	Horn et al., 1972; Lippolt et al., 1975; Nairn and Negendank, 1973
Eocene/ Oligocene	Hocheifel 50.3/7.0	45–23	47/351	1.0	59.1	3.4	79.5	182.6	3.8	5.0	Cantarel and Lippolt, 1977; Schmincke and Mertes, 1979; Bleil et al., 1982; this paper
Late Oligocene/ Early Miocene	Heldburg dyke swarm 50.2/10.8	42–16	6/83	11.7	57.3	9.8	75.1	152.2	10.4	14.3	Lippolt, 1982; Pohl and Soffel, 1977
	Lower Silesia 51.1/15.6	Oligocene/ Miocene (36–29)	51/290	4.8	63.9	4.4	83.6	163.9	5.6	7.0	Urry, 1936; Birkenmajer and Nairn, 1969
	Lausitz 51.0/14.8	28–24-19	23/145	20.2	62.2	5.0	74.4	125.8	6.0	7.8	Todt and Lippolt, 1975b; Nairn and Vollstädt, 1967
	Westerwald 50.5/7.9	28–22	5/14	11.3	55.4	11.9	73.3	154.2	12.1	17.0	Lippolt and Todt, 1978; Nairn, 1962

Table 4 (continued)

Epoch	Volcanic center λ/ϕ	Age	n/N	ChRM D	ChRM I	ChRM α_{95}	Pole Position λ'	Pole Position ϕ'	dp	dm	References
	Siebengebirge 50.7/7.2	26–24–19	6/17	37.4	61.9	8.1	63.7	99.2	9.7	12.5	Todt and Lippolt, 1980; (Nairn, 1960); Nairn, 1962
	Oberpfalz 50.0/12.2	29–24–19	17/235	12.6	61.7	5.9	78.8	136.6	7.0	9.1	Todt and Lippolt, 1975a; Soffel and Supalak, 1968; Pohl and Soffel, 1977
	Rhön 50.5/10.0	25–22–19	11/86	359.8	63.8	13.4	84.9	191.3	16.9	21.2	Bock and Soffel, 1971; Lippolt, 1978
Mean			7				77.6	135.1	7.2^{+}		
Middle Miocene/ Late Miocene	Kaiserstuhl 48.1/7.6	18–13	8/–	5.7	50.1	12.6	72.2	171.3	11.3	16.9	Lippolt et al., 1963; Roche and Lauer, 1964
	Vogelsberg 50.5/9.1	16–13	38/194	13.9	57.4	5.1	74.1	145.5	5.5	7.5	Harre et al., 1975; Ehrenberg et al., 1977; Angenheister, 1956; (Nairn, 1960)
	Ries Impact Crater 48.8/10.5	15	12/111	11.4	59.5	1.4	78.4	142.6	1.6	2.1	Gentner et al., 1963; Pohl, 1965
	Göttingen Region 51.4/9.8	20–~13–7	15/159	11.7	61.2	8.9	77.9	143.9	10.5	13.6	Kreutzer et al., 1973; Wedepohl, 1978; Schult, 1963, 1975
	Habichtswald 51.3/9.3	Late Miocene	4/11	357.7	66.2	19.1	86.9	218.9	25.7	31.4	Rösing, 1958; Schult, 1963
	Hegau 48.5/9.5	16–13	12/129	8.3	65.0	10.5	84.2	111.4	13.7	17.0	Lippolt et al., 1963; Horn et al., 1972; Baranyi et al., 1976; Nairn and Negendank, 1973; Mäussnest, 1979
Mean			6				79.7	151.6	6.0^{+}		
Mean for Late Oligocene/ Miocene			13				78.7	141.9	4.4^{+}		

λ, ϕ geographic latitude in °N and longitude in °E; n/N number of sites/samples; all other symbols as in Table 2. Ages given in m.y. refer only to periods for which paleomagnetic data are available, main eruptional phases are underlined (for a comprehensive review of K/Ar ages see Lippolt, 1982).

$^{+}$ Radius of the 95% confidence circle for mean pole position

ropean volcanic centers. Table 4 gives a revised and updated summary of all relevant results north and outside the Alpine-Carpathian orogenic belt for which the original data were available. In calculating mean directions and virtual geomagnetic pole positions, the following acceptibility criteria were applied:

- number of separately oriented samples per site $\geqq 2$,
- $\alpha_{95} < 25°$,
- $\lambda' > 45°$.

All results quoted as unreliable in the original papers were also rejected. With exception of the Vogelsberg and in part the Kaiserstuhl, only ChRM directions obtained from demagnetization treatments are included in the mean values of Table 4. Despite this minimum sampling frame, several sets of data listed are unlikely to be entirely representative for the respective volcanic province, mainly because the number of individual sites is to small.

Moreover, the paleomagnetic methods used both for data acquisition and analysis some 20 years ago when the bulk of the results was published may not always be adequate to modern standards. On the other hand, a sufficient K/Ar age control is now available almost everywhere (see review by Lippolt, 1982) which allows the calculation of separate mean VGP positions for the Late Oligocene/Early Miocene and Middle/Late Miocene periods, respectively (Table 4). Essentially, these results confirm the McElhinny (1973) APW path but very clearly deviate from the Irving (1977) data (Fig. 6). The latter include and are obviously dominated by a large number of paleomagnetic results from the Russian platform. Most of these data come from orogenic regions in the southern USSR and one might speculate, therefore, that tectonic rotations may account for the observed discrepancies in the Miocene VGP positions. Another aspect addressed by McElhinny (1973) is the mostly unsolved problem of comparing Russian work with results from western countries as very often quite different techniques are employed to elaborate paleomagnetic data.

For the Paleocene/Eocene period, a mean Western European VGP postion of 79.1° N, 173.1° E, $\alpha_{95}=6.3°$ (Fig. 6) was obtained from 11 entries of the Ottawa listings (Irving et al., 1976) which received two stars in their filter system and, therefore, should be the most reliable results presently available. The bulk of these data come from various NW European, mostly British, Lower Tertiary volcanic provinces. The Mediterranean region has not been considered. Due to the relatively large 95% confidence circle, on grounds of statistics, this pole is not significantly different from the Hocheifel VGP. Compared to the Miocene period, the most remarkable feature is its position close to the 180° meridian.

Conclusions

The mean virtual geomagnetic pole position derived from the paleomagnetic analyses of Tertiary Hocheifel volcanics shows a conspicuous agreement with an apparent polar wander path for Cenozoic Eurasia based on a large number of combined paleomagnetic results from stable continental Western Europe and the Russian and Siberian platforms (Irving, 1977; Fig. 6). In particular, the Hocheifel VGP position confirms the radiometric age range of an Eocene to Oligocene volcanic activity in this part of the Rhenish shield. However, a comparison to Western European paleomagnetic data alone would result in a much less unequivocal interpretation. A Paleocene/Eocene pole obtained from paleomagnetics of Lower Tertiary NW European volcanic fields is statistically indistinguishable from the Hocheifel VGP. As a general trend, they both follow the Eurasian APW path roughly along the 180° meridian. In clear contrast, the VGP's for Miocene Central European volcanics typically fall into the 90°–180° E longitudinal quadrant (Table 4). Their mean pole position differs by about 40° in longitude from the Hocheifel VGP. Relative to the Eurasian APW, there is also a discrepancy of some 5° in latitude.

Neglecting true polar wander, the Miocene VGP of stable continental Western Europe would indicate an average northward latitudinal motion of about 0.5° per million years over the past about 20 m.y.. In addition, two large antagonistic rotational components would be required from present to Miocene and Miocene to Oligocene/Eocene times, respectively. This hardly appears to be a realistic alternative to the Eurasian APW path of Irving (1977). As discussed above, the quality of at least some underlying paleomagnetic data tends to cast doubt on the significance of the Miocene Central European VGP. On the other hand, Watkins (1973) obtained similar results from an extensive paleomagnetic survey of the Canary Islands for this period and pointed out that a significant long-term non-dipole component in the Late Tertiary paleofield could possibly account for these effects. Whatever the mechanism distorting the Earth's field away from an axial geocentric dipole configuration may be (Wilson, 1970; Cox, 1975), according to various analyses, its existence for the past 25 m.y. seems well documented (see Coupland and Van der Voo, 1980 for references). It should not cause, however, polar errors greater than about 5° (Wilson and McElhinny, 1974). This is obviously less than is required to unravel the actual problems with the European APW path. In conclusion, therefore, we are left here with the somewhat disappointing fact that we still lack a reasonably established reference pole position when working in tectonically complex Late Tertiary terrains.

Acknowledgements. We would like to thank H.U. Worm for assistance during the field work and V. Spieß for his help with the preparation of the manuscript. Special thanks are due to Prof. Untiedt for making available the facilities of the paleomagnetic laboratory at Münster University and to Prof. Huckenholz (München) who provided unpublished data for a number of sampling sites.

The financial support by the Deutsche Forschungsgemeinschaft is gratefully acknowledged.

References

Angenheister, G.: Über die Magnetisierung der Basalte des Vogelsberges. Nachr. Akad. Wiss., Göttingen, Phys.-Math. Kl. **9**, 187–204, 1956

Baranyi, I., Lippolt, H.J., Todt, W.: Kalium-Argon-Altersbestimmungen an tertiären Vulkaniten des Oberrheingrabens. II. Eine K–Ar-Traverse vom Hegau nach Lothringen. Oberrh. Geol. Abh. **25**, 41–62, 1976

Birkenmajer, K., Nairn, A.E.M.: Palaeomagnetic investigations of the Tertiary and Quaternary igneous rocks: V. The basic Tertiary basalts of Lower Silesia, Poland. Geol. Rundsch. **58**, 697–712, 1969

Bleil, U., Pohl, J., Soffel, H.: Preliminary paleomagnetic studies of Tertiary volcanic rocks from the Hocheifel (Germany). Geol. Jahrb. **D52**, 149–161, 1982

Bock, G., Soffel, H.: Paleomagnetic investigations on igneous rocks from the Rhön, Germany. Z. Geophys. **37**, 581–587, 1971

Böhnel, H., Kohnen, H., Negendank, J., Schmincke, H.U.: Paleomagnetism of Quaternary volcanics of the East-Eifel, Germany. J. Geophys. **51**, 29–37, 1982

Cantarel, P., Lippolt, H.J.: Alter and Abfolge des Vulkanismus in der Hocheifel. N. Jahrb. Geol. Paläont. Monatsh. **1977**, 600–612, 1977

Chauduri, S.: Petrographische und geochemische Untersuchungen an den Alkaliolivinbasalten und Basaniten der südlichen Hocheifel. Ph.D. thesis, Universität Köln, 1970

Coupland, D.H., Van der Voo, R.: Long-term nondipole components in the geomagnetic field during the last 130 m.y. J. Geophys. Res. **85**, 3529–3548, 1980

Cox, A.V.: The frequency of geomagnetic reversals and the symmetry of the nondipole field. Rev. Geophys. Space Phys. **13**, 35–51, 1975

Duda, A., Schmincke, H.U.: Quaternary basanites, melilites, nephelinites and tephrites from the Laacher See area (Germany). N. Jahrb. Miner. Abh. **132**, 1–33, 1978

Duncan, R.A., Petersen, N., Hargraves, R.B.: Mantle plumes, movement of the European plate, and polar wandering. Nature **239**, 82–86, 1972

Ehrenberg, K.H., Harre, W., Kreutzer H.: Datierungen nach der K–Ar-Methode. In: Erläuterungen zur geologischen Karte von Hessen, Blatt Nr. 5721 Gelnhausen, 107–110, 1977

Fuchs, G.: Zum Eruptionsmechanismus der tertiären Hocheifel-Basalte: Der Arensberg bei Zilsdorf. Decheniana **122**, (1), 129–145, 1969

Fuller, M., Williams, I., Hoffman, K.A.: Paleomagnetic records of geomagnetic field reversals and the morphology of the transitional fields. Rev. Geophys. Space Phys. **17**, 179–203, 1979

Gentner, W., Lippolt, H.J., Schaeffer, O.A.: Das Kalium-Argon-Alter der Gläser des Nordlinger Rieses und der böhmisch-mährischen Tektite. Geochim. Cosmochim. Acta **27**, 191–200, 1963

Grünhagen, H.: Petrographische und geochemische Untersuchungen an Andesiten und Trachyten der Hocheifel. Ph.D. thesis, Universität Köln, 1964
Harre, W., Kreuter, H., Müller, P., Pucher, R., Schricke, W.: Datierungen nach der K/Ar-Methode und Paläomagnetik. In: Erläuterungen zur geologischen Karte von Hessen, Blatt Nr. 5319 Londorf, 67–73, 1975
Haverkamp, U.: Paläomagnetische Untersuchungen an quartären Vulkaniten der Westeifel. Unpubl. Diploma Thesis, University of Münster, 1980
Hoffman, K.A., Day, R.: Separation of multi-component NRM: A general method. Earth Planet. Sci. Lett. **40**, 433–438, 1978
Horn, P., Lippolt, H.J., Todt, W.: Kalium-Argon-Altersbestimmungen an tertiären Vulkaniten des Oberrheingrabens. I. Gesamtgesteinsalter. Ecl. Geol. Helv. **65**, 131–165, 1972
Huckenholz, H.G.: Der petrogenetische Werdegang der Klinopyroxene in den tertiären Vulkaniten der Hocheifel. I. Die Klinopyroxene der Alkaliolivinbasalt-Trachyt-Assoziation. Contrib. Mineral. Petrol. **11**, 138–195, 1965a
Huckenholz, H.G.: Der petrogenetische Werdegang der Klinopyroxene in den tertiären Vulkaniten der Hocheifel. II. Die Klinopyroxene der Basanitoide. Contrib. Mineral. Petrol. **11**, 415–448, 1965b
Huckenholz, H.G.: Der petrogenetische Werdegang der Klinopyroxene in den tertiären Vulkaniten der Hocheifel. III. Die Klinopyroxene der Pikritbasalte (Ankaramite). Contrib. Mineral. Petrol. **12**, 73–95, 1966
Illies, J.H., Prodehl, C., Schmincke, H.U., Semmel, A.: The Quaternary uplift of the Rhenish shield in Germany. Tectonophysics **61**, 197–225, 1979
Irving, E.: Drift of the major continental blocks since the Devonian. Nature **270**, 304–309, 1977
Irving, E., Tanczyk, E., Hastie, J.: Catalogue of paleomagnetic directions, 5, Cenozoic results. Geomag. Ser. **10**, Department of Energy, Mines and Resources, Ottawa, Canada, 1976
Jäger, G.: Paläomagnetische Untersuchungen im quartären Vulkanfeld der Westeifel. Unpubl. Diploma Thesis, University of Münster, 1982
Knetsch, G.: Vulkane der Hohen Eifel. In: Die vulkanische Eifel, J. Frechen, M. Hopmann, and G. Knetsch, eds. Bonn: Stollfuss 1959
Kohnen, H., Westkämper, H.: Palaeosecular variation studies of the Brunhes Epoch in the volcanic province of the East-Eifel, Germany. J. Geophys. **44**, 545–555, 1978
Kreutzer, H., Besang, C., Harre, W., Müller, P., Ulrich, H.J., Vinken, R.: K – Ar-Datierungen an jungtertiären Basalten aus dem Vogelsberg und aus dem Raum zwischen Kassel und Göttingen. Fortschr. Mineral. **50**, Bh. 3, 10–11, 1973
Lippolt, H.J.: K – Ar-Untersuchungen zum Alter des Rhön-Vulkanismus. Fortschr. Mineral. **56**, Bh. 1, 85, 1978
Lippolt, H.J.: K/Ar age determinations and the correlation of Tertiary volcanic activity in Central Europe. Geol. Jahrb. **D52**, 113–135, 1982
Lippolt, H.J., Baranyi, I., Todt, W.: Die Kalium-Argon-Alter der postpermischen Vulkanite des nordöstlichen Oberrheingrabens. Aufschluss, Sb. **27**, 205–212, 1975
Lippolt, H.J., Gentner, W., Wimmenauer, W.: Altersbestimmungen nach der Kalium-Argon-Methode an tertiären Eruptivgesteinen Südwestdeutschlands. Jahrb. Geol. L.-Amt Baden-Württ. **6**, 507–538, 1963
Lippolt, H.J., Todt, W.: Isotopische Altersbestimmungen an Vulkaniten des Westerwaldes. N. Jahrb. Geol. Paläont. Monatsh. **1978**, 332–352, 1978
Mäussnest, O.: Beitrag zum Gesteinsmagnetismus der basaltischen Förderprodukte in der Hegau-Vulkanprovinz. Oberrh. Geol. Abh. **28**, 73–77, 1979
McElhinny, M.: Palaeomagnetism and plate tectonics. Cambridge: Cambridge University Press, 1973
Nairn, A.E.M.: Paleomagnetic results from Europe. J. Geology, **68**, 285–306, 1960
Nairn, A.E.M.: Paleomagnetic investigations of the Tertiary and Quaternary igneous rocks. 1. Preliminary collections in the Eifel, Siebengebirge and Westerwald. Notizbl. Hess. L.-Amt Bodenforsch. **90**, 412–424, 1962
Nairn, A.E.M., Negendank, J.: Palaeomagnetic investigations of the Tertiary and Quaternary igneous rocks: VII. The Tertiary rocks of Southwest Germany. Geol. Rundsch. **62**, 126–137, 1973
Nairn, A.E.M., Vollstädt, H.: Paleomagnetic investigations of Tertiary and Quaternary rocks: IV. The Tertiary volcanics of the Lausitz area, Germany. Geol. Rundsch. **57**, 385–402, 1967
Ness, G., Levi, S., Couch, R.: Marine magnetic anomaly timescales for the Cenozoic and Late Cretaceous: A précis, critique, and synthesis. Rev. Geophys. Space Phys. **18**, 753–770, 1980
Pohl, J.: Die Magnetisierung der Suevite des Rieses. N. Jahrb. Mineral. Monatsh. **1965**, 268–276, 1965
Pohl, J., Soffel, H.: Palaeomagnetic and rock magnetic investigation of Tertiary volcanics in Northern Bavaria. J. Geophys. **42**, 459–474, 1977
Roche, A., Lauer, J.P.: La direction de l'aimantation de formations volcaniques du Kaiserstuhl et l'évolution du champ magnétique terrestre au Miocène. C.R. Acad. Sc. Paris **258**, 1580–1582, 1964
Rösing, F.: Erläuterungen zur geologischen Karte von Hessen, Blatt Nr. 4622 Kassel-West, 1958
Ryall, P.J.C., Hall, J.M., Clark, J., Milligan, T.: Magnetization of oceanic crustal layer 2 – results and thoughts after DSDP Leg 37. Can. J. Earth Sci. **14**, 684–706, 1977
Schult, A.: Über die Magnetisierung der Basaltvorkommen in der Umgebung von Göttingen. Z. Geophys. **29**, 1–20, 1963
Schult, A.: Die Selbstumkehr der remanenten Magnetisierung beobachtet an einigen tertiären Alkali-Basalten. Habil. Thesis, Universität München, 1975
Schmincke, H.U., Mertes, H.: Pliocene and Quaternary volcanic phases in the Eifel volcanic fields. Naturwissenschaften **66**, 614–615, 1979
Soffel, H., Supalak, P.: Paläomagnetische Messungen am Basalt des Parkstein bei Weiden (Bayern). Z. Geophys. **34**, 287–296, 1968
Todt, W., Lippolt, H.J.: K – Ar-Altersbestimmungen an Vulkaniten bekannter paläomagnetischer Feldrichtung: I. Oberpfalz und Oberfranken. J. Geophys. **41**, 43–61, 1975a
Todt, W., Lippolt, H.J.: K – Ar-Altersbestimmungen an Vulkaniten bekannter paläomagnetischer Feldrichtung: II. Sachsen. J. Geophys. **41**, 641–650, 1975b
Todt, W., Lippolt, H.J.: K – Ar age determinations on Tertiary volcanic rocks: V. Siebengebirge, Siebengebirge-Graben. J. Geophys. **48**, 18–27, 1980
Urry, W.D.: Ages by the Helium method: II. Post-Keweenawan. N. Bull. Geol. Soc. Am. **47**, 1217–1234, 1936
Watkins, N.D.: Palaeomagnetism of the Canary Islands and Madeira. Geophys. J.R. Astron. Soc. **32**, 249–267, 1973
Wedepohl, K.H.: Der tertiäre basaltische Vulkanismus der Hessischen Senke nördlich des Vogelsbergs. Aufschluss, Sb. **28**, 156–167, 1978
Wilson, R.L.: Permanent aspects of the Earth's non-dipole magnetic field over Upper Tertiary times. Geophys. J.R. Astron. Soc. **22**, 491–504, 1970
Wilson, R.L., McElhinny, M.W.: Investigations of the large-scale paleomagnetic field over the past 25 m.y., eastward shift of the Icelandic spreading ridge. Geophys. J. R. Astron. Soc. **39**, 571–586, 1974
Zijderveld, J.D.A.: A.C. demagnetisation of rocks: analysis of results. In: Methods in palaeomagnetism, D.W. Collinson, K.M. Creer, and S.K. Runcorn, eds. Amsterdam: Elsevier Publ. Comp. 1967

Received September 28, 1983; Revised November 17, 1983
Accepted November 17, 1983